Cement and Concrete Research 42 (2012) 728–735

Contents lists available at SciVerse ScienceDirect

Cement and Concrete Research

journal homepage: http://ees.elsevier.com/CEMCON/default.asp

Combination of lignosulfonate and AMPS®-*co*-NNDMA water retention agent—An example for dual synergistic interaction between admixtures in cement

N. Recalde Lummer, J. Plank *

Technische Universität München, Chair for Construction Chemicals, Garching, Lichtenbergstraße 4, 85747, Germany

ARTICLE INFO

Article history:
Received 2 August 2011
Accepted 16 February 2012

Keywords:
Retardation (A)
Admixture (D)
Polymers (D)
Oil well cement (E)
Fluid loss additive

ABSTRACT

In this study, compatibility between Na^+ lignosulfonate retarder and CaAMPS®-*co*-NNDMA water-retention agent, two admixtures commonly used in oil well cement, was investigated. A dual synergistic effect was found which demonstrates good compatibility of both admixtures. Na^+ lignosulfonate improves the fluid loss performance of CaAMPS®-*co*-NNDMA while the latter greatly enhances the retarding effect of lignosulfonate. The mechanism behind is that in cement pore solution, Na^+ lignosulfonate forms complexes with calcium ions and then associates into negatively charged, large agglomerates (R_h~2.4 μm). These agglomerates precipitate onto the surface of cement and result in a polymer layer of low permeability. Through this mechanism, Na^+ lignosulfonate retards cement hydration by hindering the migration of water to the surface of non-hydrated cement. Similarly, retarding effectiveness of Na^+ lignosulfonate is enhanced by CaAMPS®-*co*-NNDMA, as is evidenced by prolonged cement thickening times. The effect is caused by concomitant adsorption of CaAMPS®-*co*-NNDMA and lignosulfonate Ca complexes.

1. Introduction

Lignosulfonate constitutes one of the most popular admixtures used in cementitious systems [1]. In concrete it is applied for two different purposes: plastification of stiff concrete to enhance its flowability, pourability and workability; or water reduction, which results in a concrete with good workability but a lower water/cement ratio and corresponding higher compressive strength. By far, ready-mix concrete represents the largest application for lignosulfonates [2]. Besides their plasticizing effect, lignosulfonates are also known to retard cement hydration [3]. This effect is particularly utilized in oil well cementing. There, the borehole conditions including high temperature and high pressure require proper control of the setting of cement to allow sufficient pumping time [4]. For this reason, retarders are commonly incorporated into oil well cement slurries.

Currently, five different models have been proposed to explain the working mechanism of cement retarders [5]. *Calcium complexation:* The retarder reduces the concentration of free calcium ions existing in solution either by forming insoluble precipitates or by chelating the calcium ions. This way, the formation of cement hydrates such as e.g. calcium silicate hydrates (C–S–H) is prevented [6]. *Nucleation poisoning:* The retarder inhibits the growth of initially formed nuclei of cement hydrates by occupying the reactive faces. This effect results in reduced growth of e.g. C–S–H and $Ca(OH)_2$ crystals [7]. *Surface adsorption:* The retarder adsorbs onto the partially hydrated mineral surfaces and hinders their further reaction with water [8]. *Protective layer formation:* The retarder forms a semi-permeable membrane on the surface of cement particles which decelerates the migration of water to the mineral surface. Eventually, osmosis driven diffusion of water creates a high pressure inside the protective coating and the layer bursts, allowing hydration to continue at a normal rate [9]. *Dissolution–precipitation mechanism*: Organic phosphonic acids were found to enhance the dissolution of calcium by extraction. This reaction is followed by precipitation of a layer of calcium phosphonate which binds to the surface of cement. Thus, organic phosphonic acids inhibit cement hydration by acting as a diffusion barrier to water as well as a nucleation inhibitor [10].

While lignosulfonates have been used as cement retarders for many years, their exact working mechanism is not yet fully understood. So far, it has been shown that this polymer predominately affects the hydration kinetics of tricalcium silicate ($3CaO \cdot SiO_2$, commonly abbreviated as C_3S) which represents the main cement constituent, and that it extends the osmosis driven dormant/induction period of cement hydration [11,12]. Upon contact with water, C_3S will form C–S–H phases which possess a negative surface charge. Oppositely charged Ca^{2+} ions which are present in the cement pore solution in abundant quantity will immediately adsorb and form an ion layer on the surface of this C–S–H gel. It has been postulated that anionic lignosulfonates, through their sulfonate and hydroxyl groups, adsorb onto this Ca^{2+} ion layer and, consequently, coat the C–S–H phases with a less water-permeable layer. Thus, further hydration is slowed down by this waterproofing effect [13,14].

---

* Corresponding author. Tel.: +49 89 289 13151; fax: +49 89 289 13152.
E-mail address: sekretariat@bauchemie.ch.tum.de (J. Plank).

0008-8846/$ – see front matter © 2012 Elsevier Ltd. All rights reserved.
doi:10.1016/j.cemconres.2012.02.009

An important group of polymers which are added to oil well cement are so-called fluid loss additives (FLAs). These are water-retention admixtures which prevent uncontrolled loss of water from the slurry while it is being pumped under pressure along porous formations. Compared to the dry-mix mortar and concrete industry, the oil field typically uses more sophisticated admixtures because of the demand for high temperature stability (up to 260 °C). Anionic 2-acrylamido-2-methylpropane sulfonic acid (AMPS®)-based synthetic copolymers present a common group of high temperature stable FLAs. Through adsorption on positively charged surface sites of cement hydrates, these copolymers reduce filter cake permeability and provide low fluid loss of the slurry (adsorptive working mechanism) [15–17]. While the AMPS®-based copolymers work excellent when being the sole admixture, their effectiveness can diminish significantly when other polymers possessing either a higher anionic charge or stronger anchor groups are also present in the slurry. For example, it has been shown that the presence of a dispersant such as acetone–formaldehyde–sulfite (AFS) polycondensate or of the anti-free water agent welan gum (a microbial biopolymer) negatively impact the performance of this polymer [18,19]. As a result of competitive adsorption, decreased FLA adsorption on cement and consequently poor water retention ability and increased fluid loss were observed for the AMPS® copolymer. Such examples are indicative of the complexity of multi-admixture systems and demonstrate the importance of admixture compatibility there.

In modern building materials, combinations of several admixtures are frequently used. Such combinations are especially common in dry-mix mortar formulations like cementitious tile adhesives (CTAs) or self-leveling underlayments (SLUs) [20,21]. For example, SLUs contain superplasticizer, retarder and redispersible latex powder. Formulators and applicators are familiar with the phenomenon that some admixtures perturb the effectiveness of others.

The aim of this investigation was to study potential interactions occurring between Na^+ lignosulfonate (Na–LS) retarder and a water-retention admixture composed of 2-acrylamido-2-methylpropane sulfonic acid and *N,N*-dimethyl acrylamide (CaAMPS®-*co*-NNDMA) in cement. Performance of these two polymers was compared when being used individually and in combination. For this purpose, rheology, fluid loss, thickening time and compressive strength development of cement slurries containing Na–LS and CaAMPS®-*co*-NNDMA, respectively, were determined at 80 °C. To understand the mechanism behind a potential interaction, adsorbed amounts of Na^+ lignosulfonate and CaAMPS®-*co*-NNDMA on cement were measured individually and in combination. Furthermore, calcium binding capability, particle size distribution and anionic charge amount of Na^+ lignosulfonate were determined in cement pore solution. Based upon this data, a model for the interaction occurring between both polymers is proposed.

2. Materials and methods

2.1. Materials

2.1.1. Oil well cement

An API Class G oil well cement ("*black label*" from Dyckerhoff AG, Wiesbaden, Germany) corresponding to American Petroleum Institute (API) Specification 10A was used [22]. Its clinker composition was determined through powder XRD technique using *Rietveld* refinement. The amounts of gypsum ($CaSO_4 \cdot 2H_2O$) and hemi-hydrate ($CaSO_4 \cdot 1/2H_2O$) present in the cement sample were measured by thermogravimetry. Free lime (CaO) was quantified using the extraction method established by *Franke* [23]. According to the method described by *Blaine*, its specific surface area was found at 3058 cm^2/g. The specific density of this sample was 3.18 kg/L, as measured by Helium pycnometry. The particle size distribution of the cement sample was determined employing a laser-based particle size analyzer. Its d_{50} value was 11 μm (see Table 1).

2.1.2. CaAMPS®-co-NNDMA fluid loss polymer

Laboratory grade 2-acrylamido-2-methylpropanesulfonic acid (AMPS® monomer 2404 from Lubrizol, Rouen, France) and *N,N*-dimethyl acrylamide (NNDMA from Sigma-Aldrich, München, Germany) were used as obtained. The AMPS®-based fluid loss additive was synthesized from these monomers by free-radical polymerization in deionized water at 60 °C using sodium persulfate (Sigma-Aldrich, München, Germany) as initiator. The reaction was carried out for 2 h under nitrogen atmosphere providing an odorless solution with yellowish color and honey-like viscosity. The chemical structure of CaAMPS®-*co*-NNDMA fluid loss polymer is shown in Fig. 1. The *Brookfield* viscosity of an aqueous solution containing 17 wt.% of the FLA was 13,600 mPa·s, as measured at 27 °C. For further characterization, the polymer was dialyzed and freeze dried. Fig. 2a shows that the FT-IR spectrum of CaAMPS®-*co*-NNDMA displays N–H and O–H stretching bands at 3319 cm^{-1}, a C═O stretching band at 1612 cm^{-1}, a N–H bending band at 1542 cm^{-1}, a C–H bending band of geminal dimethyl groups at 1405 cm^{-1}, S═O stretching bands at 1177 and 1038 cm^{-1}, and a S–O stretching band at 621 cm^{-1}. GPC analysis produced molecular weights for the FLA of $1.9 \cdot 10^6$ g/mol (M_w, ±2%) and $1.2 \cdot 10^6$ g/mol (M_n, ±1.5%), respectively. The hydrodynamic radius $R_{h(z)}$ of this polymer was found at 29 nm and its gyration radius $R_{g(z)}$ at 108 nm. According to TGA measurements presented in Fig. 3a, thermal decomposition of the CaAMPS®-*co*-NNDMA commences sharply at 330 ± 10 °C. In cement pore solution, CaAMPS®-*co*-NNDMA provided a specific anionic charge amount of −370 C/g.

2.1.3. Na^+ lignosulfonate cement retarder

A commercial sample (HR-5® from Halliburton, Houston, Texas, USA) was used as obtained. The general chemical structure of this anionic cement retarder which is a semi-synthetic product based on native lignin obtained from wood and therefore ill-defined in its composition is presented in Fig. 4. The *Brookfield* viscosity of an aqueous solution containing 40 wt.% Na–LS was 32 mPa·s, as measured at 27 °C. The IR spectrum of Na^+ lignosulfonate displayed a broad band from 3600 to 3300 cm^{-1} corresponding to hydroxyl groups in phenolic and carboxylic acids (see Fig. 2b). In the fingerprint region (1900–800 cm^{-1}) the main absorptions appear at 1600 to 1500 cm^{-1} (C═C skeletal vibrations), 1470–1430 cm^{-1} (C–H deformation combined with aromatic ring vibrations), 1260 cm^{-1} (C═O stretch), 1200 cm^{-1} (C–C, C–O and C═O stretching), 1120 cm^{-1} (C–H in plane deformation), 850 and 780 cm^{-1}, respectively (C–H out-of-plane deformations), and 610 cm^{-1} (S–O stretching vibration). The molecular weight (M_w, ±2%) of this

Table 1
Phase composition (Q-XRD, *Rietveld*), specific density, specific surface area (*Blaine*) and d_{50} value of API Class G oil well cement sample.

C_3S (wt.%)	C_2S (wt.%)	C_3A_c (wt.%)	C_4AF (wt.%)	Free CaO (wt.%)	$CaSO_4 \cdot 2H_2O$ (wt.%)	$CaSO_4 \cdot 0.5 H_2O$ (wt.%)	$CaSO_4$ (wt.%)	Specific density (kg/L)	Specific surface area (cm^2/g)	d_{50} Value (μm)
59.6	22.8	1.2	13.0	<0.3	2.7[a]	0.0[a]	0.7	3.18	3058	11 ± 1.1

C_3S: tricalcium silicate ($Ca_3(SiO_4)O$); C_2S: dicalcium silicate (Ca_2SiO_4); C_3A_c: cubic modification of tricalcium aluminate ($Ca_9Al_6O_{18}$); C_4AF: tetra calcium aluminate ferrite ($Ca_4Al_2Fe_2O_{10}$).

[a] Measured by thermogravimetry.

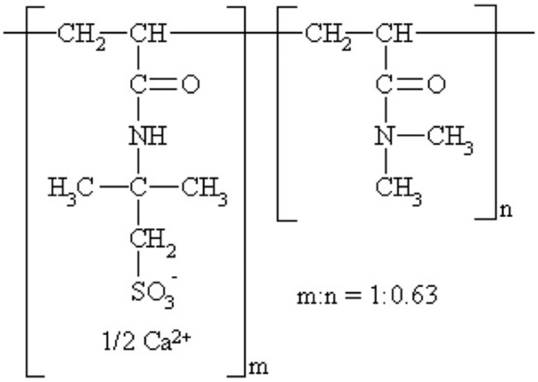

Fig. 1. Chemical structure of CaAMPS®-*co*-NNDMA fluid loss additive.

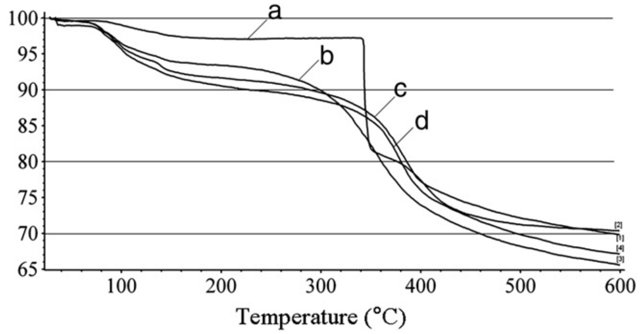

Fig. 3. TGA spectra of a: CaAMPS®-*co*-NNDMA fluid loss additive, b: pure Na^+ lignosulfonate retarder (Na–LS), c: LS Ca agglomerate, d: Na–LS/Ca^{2+}/CaAMPS®-*co*-NNDMA.

sample was $8.5 \cdot 10^4$ g/mol, the degree of sulfonation was ~0.3–0.4 as quoted by the supplier, and the sodium content was 10.1 wt.% (elemental analysis). According to TGA measurements (see Fig. 3b), thermal decomposition of Na^+ lignosulfonate gradually commences at 260 ± 10 °C. In cement pore solution, the specific anionic charge amount of Na–LS was measured to be −210 C/g.

2.2. Cement characterization

Phase composition of the cement sample was obtained by X-ray powder diffraction using a Bruker axs D8 Advance instrument from Bruker, Karlsruhe, Germany with Bragg–Bretano geometry. Topas 3.0 software was used to quantify the amounts of individual phases present in the sample by following *Rietveld's* method of refinement [24]. The instrument was equipped with a scintillation detector using Cu K_α ($\lambda = 1.5406$ Å) radiation with a scanning range between 5° and 80° 2θ. Specific density of the cement sample was measured on an Ultrapycnometer® 1000 (Quantachrome Instruments, Boynton Beach, USA). The specific surface area of the sample was determined using a *Blaine* instrument (Toni Technik, Berlin, Germany). The average particle size (d_{50} value) was obtained from a laser-based particle size analyzer (1064 instrument from Cilas, Marseille, France).

2.3. Polymer characterization

Solids content of the synthesized FLA was determined using an infrared drying balance (MA35 from Sartorius AG, Göttingen, Germany) which dried the polymer solution for 10 min at 110 °C. The value presented is the average obtained from three separate measurements. Dialysis of CaAMPS®-*co*-NNDMA was carried out in deionized water at room temperature for 5 days using membranes with a molecular weight cut off value (MWCO) of 50,000 Da (Spectra/Pro® Dialysis Membrane MWCO 50,000 from Spectrum Laboratories Inc., Rancho Dominguez, USA). Employing an ALPHA 1–4 LD plus apparatus (from Martin Christ Gefriertrocknungsanlagen GmbH, Osterode am Harz, Germany), the FLA was freeze dried for 6 h at a final pressure of 0.1 mbar.

Viscosity of the polymer solutions (FLA: 17 wt.%; Na–LS: 40 wt.%) was determined using a *Brookfield* viscometer (Model HA from Brookfield Engineering Labs. Inc, Middleboro, USA) equipped with # H1 spindle for Na–LS and # 7 spindle for CaAMPS®-*co*-NNDMA, respectively. Measurements were carried out at 100 rpm and room temperature. By multiplying the dimensionless reading with the correspondent factor, the viscosity in mPa·s was obtained.

Size exclusion chromatography (Waters Alliance 2695 from Waters, Eschborn, Germany) equipped with RI detector 2414 (Waters, Eschborn, Germany) and an 18 angle dynamic light scattering detector (Dawn EOS from Wyatt Technologies, Clinton, USA) was used. CaAMPS®-*co*-NNDMA was separated on a precolumn and two Aquagel-OH 60 columns (Polymer Laboratories, distributed by Varian, Darmstadt, Germany). Molecular weights (M_w and M_n) and radii ($R_{h(z)}$ and $R_{g(z)}$) of the FLA were determined using a 0.2 M aqueous $NaNO_3$ solution (adjusted to pH 9.0 with NaOH) as an eluant at a flow rate of 1.0 mL/min. The value of dn/dc used to calculate M_w and M_n was 0.156 mL/g (value for polyacrylamide) [25].

Infrared spectra of liquid polymer solution were measured with an attenuated total reflectance Fourier transform spectrophotometer (ATR-FTIR) (Vertex 70 from Bruker Optics, Karlsruhe, Germany). It was acquired in transmittance mode on a Diamond ATR crystal cell (MPV—Pro from Harrich Scientific Products, Pleasantville, USA) by accumulation of 128 scans with a resolution of 4 cm^{-1} and a spectral range of 4000–350 cm^{-1}. Thermal stability of the polymers was investigated by thermogravimetry using a NETZSCH STA 409 CD instrument

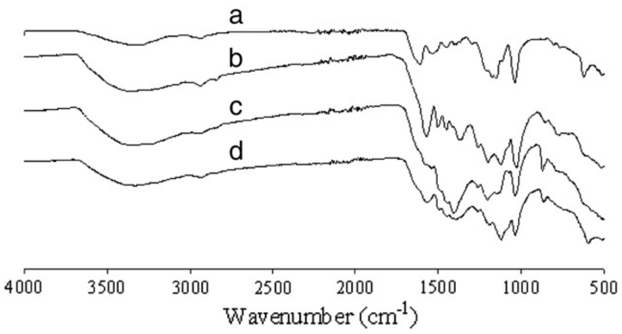

Fig. 2. Powder FT-IR spectra of a: CaAMPS®-*co*-NNDMA fluid loss additive, b: pure Na^+ lignosulfonate retarder (Na–LS), c: LS Ca agglomerate, d: Na–LS/Ca^{2+}/CaAMPS®-*co*-NNDMA.

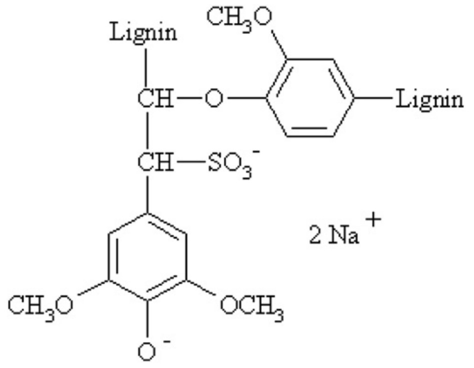

Fig. 4. General chemical structure of Na^+ lignosulfonate cement retarder.

(NETZSCH-Gerätebau GmbH, Selb, Germany) in an argon atmosphere at a heating rate of 10 °C/min.

The specific anionic charge amount of the polymers used in this study was determined in 0.1 M NaOH (pH = 13) in the presence or absence of calcium ions (0.6 g/L Ca^{2+} added as $CaCl_2 \cdot 2H_2O$), in 0.002 M NaOH (pH = 9.0) as a function of the calcium concentration present in the solvent (Ca^{2+} stepwise added as 0.1 M $CaCl_2 \cdot 2H_2O$ aqueous solution), or in cement pore solution at room temperature using a PCD 03 pH apparatus (BTG Mütek GmbH, Herrsching, Germany). Charge titration was carried out according to a literature description employing a 0.001 N solution of laboratory grade poly(diallyl dimethylammonium chloride) from BTG Mütek GmbH, Herrsching, Germany as cationic polyelectrolyte [26]. The values presented in this study are the average obtained from three different measurements. The deviation of this method was found to be ±5 C/g.

Particle size distribution (d_{50} value) of the agglomerated lignosulfonate Ca complexes was measured in 0.002 M NaOH (pH = 9.0) as a function of the calcium concentration present in the solvent (Ca^{2+} added stepwise as 0.1 M aqueous solution of $CaCl_2 \cdot 2H_2O$ to 0.2 g/L Na^+ lignosulfonate) using a dynamic light scattering particle size analyzer (LB-550 from Horiba, Irvine, USA).

2.4. Cement paste testing

2.4.1. Cement slurry preparation

Cement slurries were prepared in accordance with the procedures set forth in *Recommended Practice for Testing Well Cements*, API Recommended Practice 10B, issued by the American Petroleum Institute [27]. The slurries were mixed at a water-to-cement (w/c) ratio of 0.44 using a blade-type laboratory blender manufactured by Waring Products Inc. (Torrington, USA). Admixture dosages are stated in % by weight of cement (bwoc). Prior to cement addition, the synthesized FLA was dissolved in deionized water. In contrast, the powdered lignosulfonate-based retarder was dry blended with the cement which was added within 15 s to the water placed in a Waring blender cup and mixed for 35 s at 12,000 rpm. To ensure homogeneous consistency, all slurries were stirred in an atmospheric consistometer (model 1250 from Chandler Engineering, Tulsa, USA) for 20 min at 80 °C. The pore solution of the cement slurry prepared without polymer addition was produced by vacuum filtration (12 mbar) using a diaphragm vacuum pump (Vacuubrand GmbH, Wertheim, Germany).

2.4.2. Compressive strength analysis

The compressive strength of hardening cement samples can be estimated ultrasonically. The ultrasonic cement analyzer (model 4262 Twin Cell UCA from Chandler Engineering, Tulsa, USA) used here measures the travel time of ultrasonic energy through a cement sample while it cures under specific temperature and pressure conditions. The sonic strength is correlated to the transit time (reciprocal of ultrasonic velocity) using an empirical relationship initially established from mechanical compressive strength and transit time data for various slurry systems [28]. Immediately after mixing in the Waring blender, the respective slurry was poured into a cell of the UCA and heated up to 80 °C under a differential pressure of 200 bar (heating rate 1.3 °C/min). All measurements were carried out until a compressive strength of at least 3.4 N/mm^2 (this value corresponds to 500 psi and is commonly accepted by the industry to be sufficient to support the casing placed in the borehole to allow drilling ahead) was reached.

2.4.3. Determination of the thickening time

The time span during which the cement slurry remained in a pumpable, fluid state was determined using a high temperature, high pressure (HTHP) consistometer (model 8240 from Chandler Engineering, Tulsa, USA). This instrument is capable of measuring the consistency (viscosity) of cement slurries under conditions of high temperature (up to 315 °C) and high pressure (up to 2750 bar). Slurry viscosity was measured in Bearden Units of Consistency (Bc), a dimensionless unit obtained from the torque of a paddle rotating in the hydrating cement slurry, with no direct conversion factor to common units for viscosity. In this test, setting and solidification of cement is evidenced by an increase of slurry viscosity from <20 Bc for the slurry as prepared to a value of 70 Bc and higher. At this point, the curing cell has to be depressurized, cooled and dismantled immediately to avoid destruction of the equipment. A value of 70 Bc is generally considered to be the maximum pumpable consistency. Here, effectiveness of Na^+ lignosulfonate cement retarder was tested in absence and presence of CaAMPS®-*co*-NNDMA FLA at 80 °C and 400 bar (heating rate 1.2 °C/min; pressure rate 8.9 bar/min).

2.4.4. Rheology measurement

For rheological measurements of cement slurries, a Couette-type coaxial cylinder rotational viscometer, FANN 35SA (Fann Instruments Company, Houston, Texas, USA) equipped with R1 rotor sleeve (rotor radius: 18.4 mm), B1 bob (radius: 17.3 mm, height: 38.0 mm) and F1 torsion spring was used. The values of the viscometer reading were recorded for 6 speeds of the rotor (3, 6, 100, 200, 300, 600 rpm). The value of shear stress τ (Pa) was calculated by including the torsion spring factor (N cm/degree), the shear stress constant for the effective bob surface (cm^{-3}), and the shear rate constant (s^{-1}/rpm) [29].

2.4.5. Water retention test

Static fluid loss was measured at 80 °C using a 500 mL high temperature, high pressure (HTHP) stainless steel filter press cell manufactured by OFI Testing Equipment Inc. (Houston, Texas, USA). Design of this HTHP filter cell and its operation are described in detail in a norm issued by the American Petroleum Institute (API) [27]. After pouring the homogenized slurry obtained from the atmospheric consistometer into the HTHP cell, a heating jacket (OFI Testing Equipment Inc., Houston, Texas, USA) was used to adjust the test temperature. Then, a differential pressure of 70 bar N_2 was applied at the top of the cell. Filtration proceeded through a 22.6 cm^2 (3.5 in^2) mesh metal sieve placed at the bottom of the cell. The fluid volume collected within 30 min was doubled as described by API RP 10B and regarded as API fluid loss of the corresponding slurry [27]. The values reported for the respective API fluid loss test represents the average obtained from three separate measurements. The maximum deviation of the fluid loss value was ±10 mL/30 min.

2.4.6. Adsorption of CaAMPS®-co-NNDMA

Adsorbed amount of the AMPS®-based fluid loss additive was determined from the filtrate collected in the respective fluid loss test. Generally, the depletion method was applied, i.e. it was assumed that the decrease in the polymer concentration before and after contact with cement solely resulted from adsorption on the mineral surface. This assumption was confirmed through a solubility test. For this purpose, 11.4 g/L of CaAMPS®-*co*-NNDMA (this concentration correlates to a polymer dosage of 0.5% bwoc) was dissolved in cement pore solution and stored for 1 day. No precipitation of CaAMPS®-*co*-NNDMA was observed. Achievement of adsorption equilibrium was confirmed by zeta potential values which were constant at the time of collecting the filtrate for adsorption measurement. The adsorbed amount was calculated from the difference in the equilibrium concentration of the polymer present in the liquid phase before and after adsorption (depletion method). When CaAMPS®-*co*-NNDMA was the sole polymer present in the cement filtrate, a High TOC II apparatus (Elementar, Hanau, Germany) equipped with a CO_2 detector was used to quantify polymer adsorption. Before conducting the TOC analysis, the alkaline cement filtrate containing the unadsorbed polymer was diluted with 0.1 M HCl at a ratio of 1:10 (v./v.). Final pH of the solution was 1.0.

In the binary admixture system, concentration of the AMPS®-based FLA was determined by TN analysis (High TOC II from Elementar, Hanau, Germany; equipped with NO_x detector). The depleted amount of the lignosulfonate was calculated by subtracting the concentration of the FLA from the sum of sorbed admixtures measured by TOC analysis. For this TOC analysis, the alkaline cement filtrate containing the unadsorbed polymers was diluted with 0.01 M phosphoric acid at a ratio of 1:10 (v./v.). Final pH of the solution was 7.0. Here, the maximum deviation of the adsorption measurement was found to be ± 0.1 mg polymer/g cement.

2.4.7. Zeta potential measurement

Zeta potential of cement slurries was measured at room temperature on an electro acoustic spectrometer (DT-1200 from Dispersion Technology Inc., Bedford Hills, USA) [26]. Since zeta potential was determined as a function of time (here 30 min), cement slurries were poured into the cup of the spectrometer directly after mixing without homogenization in the atmospheric consistometer. The accuracy of this method was ± 1 mV.

2.4.8. Environmental scanning electron microscopy (ESEM)

The surface of cement slurries was analyzed by an environmental scanning electron microscope (XL 30 ESEM FEG from FEI Company, Eindhoven, The Netherlands) at 1.0 mbar pressure in the sample chamber. Energy dispersive X-ray spectroscopy (New XL-30 from EDAX, Mahwah, USA) was used to determine the presence of polymer agglomerates on cement at an acceleration voltage of 10,000 V.

3. Results and discussion

3.1. Interaction between Na$^+$ lignosulfonate and calcium ions

To clarify a potential interaction between Na$^+$ lignosulfonate and Ca^{2+} ions present in the pore solution of cement slurries, the concentration of dissolved Na–LS polymer was measured at high pH as a function of increased Ca^{2+} concentration (see Fig. 5). The initial Na–LS concentration in the Ca^{2+} free solution was 4.6 g/L (corresponding to a polymer dosage of 0.2% bwoc). At calcium concentrations higher than 0.2 g/L, the Na–LS concentration decreased dramatically and reached a plateau at ~0.7 g/L Ca^{2+}. There, the Na–LS concentration stabilized at approximately 1.5 g/L. This result clearly indicates that Na$^+$ lignosulfonate precipitates at calcium concentrations generally found in cement pore solutions (here ~0.6 g/L Ca^{2+}, as measured by AAS analysis). The reason behind is a strong calcium binding capability of the lignosulfonate molecule, as evidenced from measurements of its specific anionic charge amount in absence and presence of 0.6 g/L Ca^{2+} (see Table 2).

To determine the effect of calcium ions on Na$^+$ lignosulfonate more precisely, its specific anionic charge amount and particle size (d$_{50}$ value) were measured as a function of the calcium concentration present in the solvent. It was found that the anionic charge of Na–LS decreases from −389 C/g in absence of calcium to −77 C/g at 1.0 g/L Ca^{2+} (see Fig. 6). Based on this decrease in anionic charge, Na–LS binds 6.5% Ca^{2+} on its weight. Through ion exchange of Na$^+$ against Ca^{2+}, a LS Ca complex is formed which appears to be less soluble than the more dissociated Na–LS. The LS Ca complex appears to consist of several agglomerated molecules, as was evidenced by light scattering measurement (see Fig. 6) and precipitation from solution (Fig. 7). There, particle sizes of up to ~2.4 μm were found for the LS Ca complex.

Table 2
Specific anionic charge amount of Na$^+$ lignosulfonate and CaAMPS®-*co*-NNDMA, respectively, measured in absence and presence of 0.6 g/L Ca^{2+} (polymer concentration: 0.2 g/L).

Polymer	Specific anionic charge amount (C/g)		Reduction of the specific anionic charge amount by Ca^{2+}
	Water @ pH 13	Water @ pH 13 plus 0.6 g/L Ca^{2+}	
Na$^+$ lignosulfonate	389	102	74%
CaAMPS®-*co*-NNDMA	368	352	4%

Through powder FT-IR measurements, it was found that the intensity of several IR bands detected for the pure polymer varies after the formation of the LS Ca complex, indicating that structural changes occur in the lignosulfonate molecule resulting from the addition of Ca^{2+} ions. A similar effect has been reported for LS/Fe^{2+}, Fe^{3+} complexes [30]. Furthermore, thermal decomposition of the LS Ca complex commenced at ~300 °C. This temperature exceeds that of the pure polymer (~260 °C), as determined through thermogravimetry (see Fig. 3c). Thus, it becomes obvious that in cement pore solution, the lignosulfonate retarder exists in the form of large agglomerated LS Ca complexes. Also, the presence of Ca^{2+} ions increases the temperature stability of this lignosulfonate. Next, effectiveness of the LS Ca complex for cement retardation and the working mechanism behind were investigated.

3.2. Behavior of Na$^+$ lignosulfonate in cement

To quantify the retarding effect of LS Ca complex on cement hydration, the compressive strength development of cement slurries containing different dosages of lignosulfonate was determined at 80 °C (see Table 3). At increased dosages of Na–LS, the cement took substantially longer to reach the required threshold value for the compressive strength of 3.4 N/mm^2 (from ~3 h without retarder to ~35 h at a dosage of 0.5% bwoc of Na–LS).

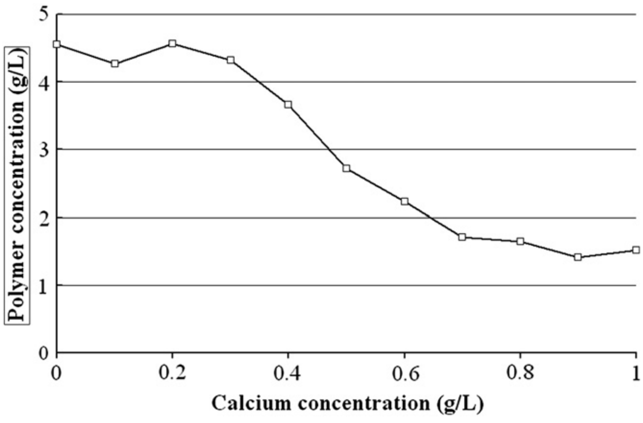

Fig. 5. Concentration of solved Na$^+$ lignosulfonate as a function of Ca^{2+} concentration, measured in aqueous solution (pH = 9.0) by TOC method at 27 °C.

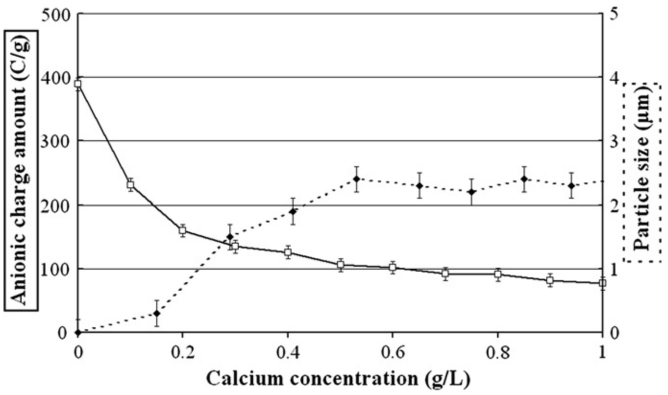

Fig. 6. Specific anionic charge amount and particle size (d$_{50}$ value) of Na$^+$ lignosulfonate as a function of the calcium concentration present in the solvent, measured at 27 °C (polymer concentration 0.5 g/L).

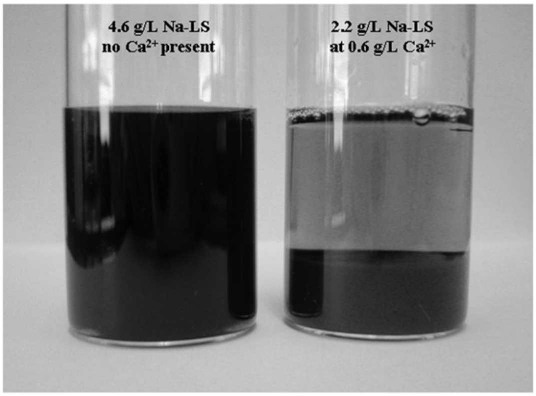

Fig. 7. Images of Na–LS solution (left) and Na–LS solution after addition of 0.6 g/L Ca^{2+} at pH = 13 (right), showing precipitation of agglomerated LS Ca complexes.

Zeta potential and rheological measurements of cement slurries conducted at increasing lignosulfonate dosages confirm adsorption of the LS Ca complex on cement (see Table 4). There, it is shown that ~0.4% bwoc of lignosulfonate, the zeta potential values stabilize and rheology of the cement slurry does not decrease further. Both observations instigate that at this lignosulfonate dosage, complete coverage of the cement surface (state of saturated adsorption) is achieved.

This model is supported by ESEM microscopy performed on cement slurries containing 0.2% bwoc of Na–LS. They show a layer of polymer distributed heterogeneously across the surface of cement, as evidenced by variations in the carbon content. Using energy dispersive X-ray spectroscopy (EDX) carbon contents between ~8 and 20% were found (see Fig. 8). Apparently, Na^+ lignosulfonate retards cement hydration by forming LS Ca complexes which precipitate onto the surface of cement. The heterogeneous distribution of the LS Ca complex is owed to variations in the surface charge of the different cement hydrates. Through this mechanism, the access of water to these sites is blocked and further growth of the cement hydrates is inhibited. The higher the amount of polymer precipitated on the surface, the greater the retardation. Next, interaction between the lignosulfonate retarder and a CaAMPS®-*co*-NNDMA fluid loss additive in cement will be presented.

3.3. Effect of Na^+ lignosulfonate on CaAMPS®-co-NNDMA

Because of the high tendency of the lignosulfonate to chelate calcium ions resulting in LS Ca complexes and agglomerates, the question arises whether anionic CaAMPS®-*co*-NNDMA, via its sulfonate groups, may also interact electrostatically with Ca^{2+} ions present on the surface of the LS agglomerates. Such interaction would reduce the concentration of freely dissolved FLA molecules in the solution. To investigate, the concentration of solved CaAMPS®-*co*-NNDMA was determined in 0.1 M NaOH (pH = 13) containing 11.4 g/L fluid loss additive (this concentration correlates to a polymer dosage of 0.5% bwoc), 4.6 g/L retarder, and 0.6 g/L Ca^{2+}. After vacuum filtration using a blue ribbon filter paper, a CaAMPS®-*co*-NNDMA concentration of only 5.4 g/L was detected, confirming that some FLA molecules adsorb onto the large LS Ca agglomerates. The FT-IR spectrum of the LS Ca complex and the thermogravimetric results were only slightly influenced by the presence of CaAMPS®-*co*-NNDMA, thus indicating their mutual interaction to be weak and physical in nature (see Figs. 2c, d and 3c, d, respectively). Next, the anionic charge and the size of particles existing in the binary admixture system were investigated under the conditions existing in a cement slurry.

Table 3
Compressive strength development of cement slurries containing increasing dosages of Na^+ lignosulfonate cement retarder, measured at 80 °C and 200 bar (w/c = 0.44).

Dosage of Na–LS (% bwoc)	Time to reach a compressive strength of 3.4 N/mm^2 at 200 bar (hh:mm)
0	02:40
0.1	04:20
0.2	07:50
0.3	12:40
0.4	21:30
0.5	34:50

Table 4
Zeta potential and rheology (shear stress) of cement slurries containing different dosages of Na^+ lignosulfonate, measured at 27 °C and 80 °C, respectively (w/c = 0.44).

Dosage of Na–LS (% bwoc)	Zeta potential at 27 °C (mV)	Shear stress (Pa) at different shear rates (s^{-1}) and 80 °C					
		1022	511	340	170	10.2	5.1
0	−5	93	82	75	64	20	17
0.1	−12	63	48	44	39	13	11
0.2	−15	47	38	34	30	11	9
0.3	−16	28	17	14	11	6	4
0.4	−17	21	9	6	4	2	2
0.5	−17	20	7	5	4	1	1

As shown before, in cement pore solution Na–LS is negatively charged (−210 C/g) and becomes very voluminous in presence of Ca^{2+} (~2.4 μm). In contrast, CaAMPS®-*co*-NNDMA exhibits a higher anionic chare amount (−370 C/g) and a smaller size ($R_{h(z)}$ = 29 nm). Thus, when both polymers are present in a cement slurry, the higher anionic charge density as well as the smaller hydrodynamic radius of CaAMPS®-*co*-NNDMA should result in preferred adsorption of the FLA on cement as a result of higher electrostatic attraction and a gain in entropy owed to the high molecular weight.

To clarify, effectiveness of the fluid loss polymer was tested in the binary admixture system. At first, the fluid loss of a cement slurry containing only Na^+ lignosulfonate at a dosage of 0.2% bwoc at 80 °C was determined. There, a calculated API fluid loss value of 1500 mL/30 min was found. Such value is considered to present extremely poor water retention. Apparently, the voluminous agglomerates formed by the LS Ca complexes do not provide substantial fluid loss control to cement slurries. It can be speculated that while these agglomerates are large in size, they exhibit a gel-like, soft consistency and are highly compressible. Thus, those swollen, hydrated polymer complexes cannot exercise much physical plugging effect. Next, the relationship between HTHP fluid loss and the amount of CaAMPS®-*co*-NNDMA

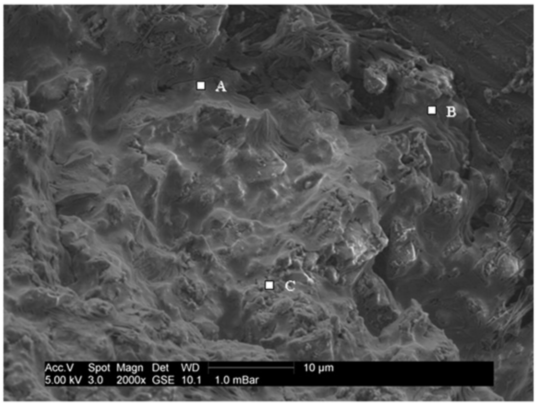

Fig. 8. ESEM image of the surface of a cement slurry containing 0.2% bwoc of Na^+ lignosulfonate, analyzed after mixing at room temperature (w/c = 0.44). Area for EDX measurements (1 μm × 1 μm) indicated by white squares. Carbon contents (%): A = 19; B = 11; C = 8.

adsorbed on cement was determined at 80 °C in the absence and presence of 0.2% bwoc of Na^+ lignosulfonate.

When 0.5% bwoc of CaAMPS®-*co*-NNDMA was added as the sole admixture to the cement slurry, the adsorbed amount was 4.2 mg FLA/g cement which produced an API fluid loss of 100 mL/30 min. In the binary system containing 0.5% bwoc of FLA and 0.2% bwoc of the lignosulfonate, the adsorbed amount of CaAMPS®-*co*-NNDMA was only slightly increased by the presence of Na–LS (from 4.2 cement to 4.4 mg FLA/g cement). Opposite to this minor effect, the resulting fluid loss decreased significantly from 100 to 60 mL/30 min (see Fig. 9). The slightly increased adsorption cannot explain such huge improved effect. Instead, it can be assumed that some of the LS Ca complexes interact with CaAMPS®-*co*-NNDMA already adsorbed on cement within the pores of the cement filter cake. This effect leads to a further decrease in filter cake permeability and hence to improved FLA performance. Furthermore, it was found that the polymer layer provided by the LS Ca complexes become much more dense in the presence of CaAMPS®-*co*-NNDMA, as will be discussed later. This way, a synergistic effect between CaAMPS®-*co*-NNDMA and lignosulfonate with respect to cement fluid loss control is achieved.

The following experiments investigate whether this synergistic interaction between CaAMPS®-*co*-NNDMA and Na–LS also enhances the retarding effect of lignosulfonate.

3.4. Effect of CaAMPS®-co-NNDMA on Na^+ lignosulfonate

As shown before, Na^+ lignosulfonate retards cement hydration by precipitation onto the cement surface. This process may be perturbed by the presence of CaAMPS®-*co*-NNDMA. Competitive interaction between both polymers for limited adsorption sites may lead to reduced coverage of the cement surface with retarder. To verify this concept, rheology measurements of cement slurries prepared with 0.5% bwoc of CaAMPS®-*co*-NNDMA were conducted at 80 °C in absence and presence of 0.2% bwoc of Na^+ lignosulfonate. Additionally, the amount of Na–LS depleted in the presence of cement was determined for this binary admixture system and compared with the results obtained from a cement slurry containing only Na–LS (see Table 5).

The cement slurry prepared with CaAMPS®-*co*-NNDMA as the sole admixture possessed a relatively high viscosity, as expected. After addition of Na–LS, however, the cement slurry became more dispersed. This effect results from the adsorption/precipitation of negatively charged LS Ca complexes onto the mineral surface, causing electrostatic repulsion and steric hindrance of correspondingly charged cement particles. Here, the depleted amount of Na–LS decreased only slightly, from 1.8 mg/g cement in the absence of CaAMPS®-*co*-NNDMA to 1.5 mg/g cement in the presence of this FLA. Evidently, the presence of CaAMPS®-*co*-NNDMA does not much impact the surface coverage of cement by Na–LS.

However, the question remains whether these voluminous agglomerates also can precipitate onto or interact electrostatically with already adsorbed CaAMPS®-*co*-NNDMA. This could influence the permeability of the layer formed by the lignosulfonate and hence its retarding effectiveness. To answer this question, thickening times of cement slurries containing different Na–LS dosages were compared at 80 °C in absence and presence of CaAMPS®-*co*-NNDMA (see Table 6). Under the conditions tested here, the neat cement slurry remained pumpable only for a short period of time (59 min). With increasing dosages of Na^+ lignosulfonate, however, the thickening time increased from ~1 h without retarder to ~6 h when 0.3% bwoc of Na^+ lignosulfonate was employed. This result confirms the high retarding effectiveness of lignosulfonate. Whereas, addition of individual 0.5% bwoc FLA only marginally influenced the thickening time of the neat cement slurry (from 0:59 h in absence to 1:06 h in presence of the FLA). Thus, it becomes obvious that CaAMPS®-*co*-NNDMA exercises only a very minor retarding effect.

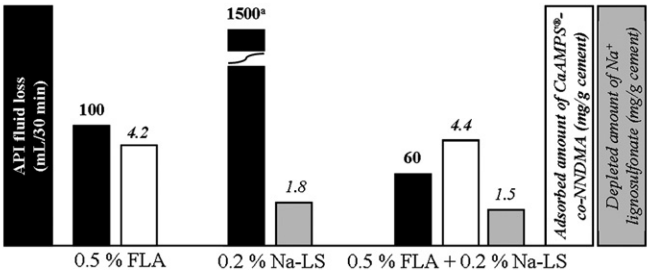

Fig. 9. API fluid loss (black bars), adsorbed amount of CaAMPS®-*co*-NNDMA (white bars) and depleted amount of Na^+ lignosulfonate (gray bar), measured in cement slurry (w/c = 0.44) at 80 °C for each admixture individually and in combination therefore. [a]Dehydration of cement slurry within less than 30 min.

Table 5
Rheology (shear stress) of cement slurries containing 0.5% bwoc of CaAMPS®-*co*-NNDMA in absence and presence of Na^+ lignosulfonate and depleted amount of Na–LS on cement, measured at 80 °C (w/c = 0.44).

Dosage of Na–LS (% bwoc)	Depleted amount of Na–LS (mg/g cement)	Shear stress (Pa) at different shear rates (s^{-1})					
		1022	511	340	170	10.2	5.1
0	0	122	91	71	45	16	16
0.2	1.5	92	63	46	28	4	2

Surprisingly, the presence of this fluid loss additive strongly enhanced the retarding effect of Na^+ lignosulfonate (from ~8 h of pumping time for a cement slurry containing 0.4% bwoc of Na^+ lignosulfonate to ~21 h for the combination with 0.5% bwoc FLA). Obviously, adsorption of CaAMPS®-*co*-NNDMA molecules onto the surface of cement further densifies the polymer layer provided by LS Ca complexes, thus enhancing the effectiveness of this retarder. Consequently, in a binary admixture system comprising of both CaAMPS®-*co*-NNDMA and Na^+ lignosulfonate, a dual synergistic effect regarding fluid loss control as well as cement retardation is observed.

4. Conclusions

In this study, compatibility between Na^+ lignosulfonate retarder and CaAMPS®-*co*-NNDMA water-retention agent, two admixtures commonly used in oil well cement, was investigated. A synergistic effect between those two admixtures was found. Na^+ lignosulfonate improves the fluid loss performance of CaAMPS®-co-NNDMA while the latter greatly enhances the retarding effect of lignosulfonate. This way, a dual synergistic effect occurs which demonstrates good compatibility of both admixtures. The mechanism behind is that in cement pore solution Na–LS forms complexes with calcium ions and then associates into large agglomerates. Those agglomerates

Table 6
Thickening time of cement slurries containing increasing dosages of Na^+ lignosulfonate in absence and presence of CaAMPS®-*co*-NNDMA, measured at 400 bar and 80 °C (w/c = 0.44).

Dosage of Na–LS (% bwoc)	Dosage of FLA (% bwoc)	Thickening time [a] (hh:mm)
0	0	00:59
	0.5	01:06
0.1	0	01:56
	0.5	02:00
0.2	0	03:28
	0.5	04:30
0.3	0	05:44
	0.5	11:52
0.4	0	08:23
	0.5	21:14

[a] Time to reach a cement consistency of 70 Bc, measured on a HTHP consistometer.

precipitate onto the surface of cement and result in a polymer layer of low permeability. Through this mechanism, Na^+ lignosulfonate retards cement hydration by hindering the migration of water to the surface of non-hydrated cement.

The study demonstrates the importance of understanding the various physico-chemical interactions between admixtures which can influence their behavior and performance. Here, a very rare example of a dual synergistic effect where both admixtures gain from the presence of the other is described. While in many cases, admixtures perturb each other which leads to decreased performance. Understanding these interactions may help to develop advanced admixtures and reduce the problem of incompatibility.

Acknowledgments

The authors wish to thank Halliburton (Houston, Texas, USA) for generously providing the sodium lignosulfonate sample.

References

[1] V.S. Ramachandran, Concrete Admixtures Handbook, 2nd Ed. Noyes Publications, Park Ridge, 1995.

[2] J. Plank, Applications of biopolymers and other biotechnological products in building materials, Appl. Microbiol. Biotechnol. 66 (2004) 1–9.

[3] B.O. Myrvold, Adsorption of lignosulphonate on cement and the hydration products of cements, Proceedings 8th CANMET/ACI International Conference on Superplasticizers and Other Chemical Admixtures in Concrete, SP-239-19, Farmington Hills, 2006, pp. 285–296.

[4] E.B. Nelson, D. Guillot, Well Cementing, Schlumberger Dowell, Sugar Land, TX, 2006.

[5] H.F.W. Taylor, Cement Chemistry, Thomas Telford, New York, 1997.

[6] V.S. Ramachandran, R. Feldman, J. Beaudoin, Concrete Science: Treatise on Current Research, Heyden and Son. Ltd., Philadelphia, 1981.

[7] N.L. Thomas, J.D. Birchall, The retarding action of sugars on cement hydration, Cem. Concr. Res. 13 (1983) 830–842.

[8] P.V. Coveney, W. Humphries, Molecular modelling of the mechanism of action of phosphonate retarders on hydrating cements, J. Chem. Soc. Faraday Trans. 92 (1996) 831–841.

[9] D.D. Double, P.C. Hewlett, K.S.W. Sing, J.F. Raffle, New developments in understanding the chemistry of cement hydration, Phil. Trans. R. Soc. Lond. A 310 (1983) 53.

[10] M. Bishop, A.R. Barron, Cement hydration inhibition with sucrose, tartaric acid, and lignosulfonate: analytical and spectroscopic study, Ind. Eng. Chem. Res. 45 (2006) 7042–7049.

[11] V.S. Ramachandran, M.S. Lowery, Conduction calorimetric investigation of the effect of retarders on the hydration of Portland cement, Thermochim. Acta 195 (1992) 373–387.

[12] M.Y.A. Mollah, W. Yu, R. Schennach, D.L. Cocke, A Fourier transform infrared spectroscopic investigation of the early hydration of Portland cement and the influence of sodium lignosulfonate, Cem. Concr. Res. 30 (2000) 267–273.

[13] N.L. Thomas, D.D. Double, Calcium and silicon concentrations in solution during the early hydration of Portland cement and tricalcium silicate, Cem. Concr. Res. 11 (1981) 675–687.

[14] J.D. Birchall, A.J. Howard, D.D. Double, Some general considerations of a membrane/osmosis model for Portland cement hydration, Cem. Concr. Res. 10 (1980) 145–155.

[15] J. Desbrières, Cement cake properties in static filtration: influence of polymeric additives on cement filter cake permeability, Cem. Concr. Res. 23 (1993) 347–358.

[16] J. Plank, A. Brandl, Y.N. Zhai, A. Franke, Adsorption behavior and effectiveness of poly(N, N-dimethylacrylamide-co-Ca 2-acrylamido-2-methylpropanesulfonate) as cement fluid loss additive in the presence of acetone-formaldehyde-sulfite dispersant, J. Appl. Polym. Sci. 102 (2006) 4341–4347.

[17] J. Plank, A. Brandl, N. Recalde Lummer, Effect of different anchor groups on adsorption behavior and effectiveness of poly(N, N-dimethylacrylamide-co-Ca 2-acrylamido-2-methylpropanesulfonate) as cement fluid loss additive in presence of acetone–formaldehyde–sulfite dispersant, J. Appl. Polym. Sci. 106 (2007) 3889–3894.

[18] J. Plank, F. Dugonjic-Bilic, N. Recalde Lummer, Modification of the molar anionic charge density of acetone–formaldehyde–sulfite dispersant to improve adsorption behavior and effectiveness in the presence of CaAMPS® co-NNDMA cement fluid loss polymer, J. Appl. Polym. Sci. 111 (2008) 2018–2024.

[19] J. Plank, N. Recalde Lummer, F. Dugonjic-Bilic, Competitive adsorption between an AMPS®-based fluid loss polymer and welan gum biopolymer in oil well cement, J. Appl. Polym. Sci. 116 (2010) 2913–2919.

[20] R. Bayer, H. Lutz, 6th Edition, Dry Mortars, Ullmann's Encyclopedia of Industrial Chemistry, 9, 2003, pp. 1–26.

[21] C. Winter, J. Plank, The European dry-mix mortar industry (Part 1 and 2), ZKG Int. 60 (6, 9) (2007) 62–69 and 58–66.

[22] American Petroleum Institute, API Specification 10A, 23rd ed American Petroleum Institute, Washington, 2002.

[23] B. Franke, Bestimmung von Calciumoxyd und Calciumhydroxyd neben wasserfreiem und wasserhaltigem Calciumsilikat, Z. Anorg. Allg. Chem. 247 (1941) 180.

[24] L.B. McCusker, R.B. Von Dreele, D.E. Cox, D. Louër, P. Scardi, Rietveld refinement guidelines, J. Appl. Crystallogr. 32 (1999) 36.

[25] M.B. Huglin, Polymer Handbook, in: J. Brandrup, E.H. Immergut (Eds.), 3rd ed., Wiley, New York, 1989.

[26] J. Plank, B. Sachsenhauser, Experimental determination of the effective anionic charge density of polycarboxylate superplasticizers in cement pore solution, Cem. Concr. Res. 39 (2009) 1–5.

[27] American Petroleum Institute, API Recommended Practice 10B, 22nd ed. American Petroleum Institute, Washington, 1997.

[28] P.P. Rao, D.L. Sutton, *Method and apparatus for nondestructive testing of cement*, US 4,259,868 (1981).

[29] K.H. Khayat, A. Yahia, Simple field tests to characterize fluidity and washout resistance of structural cement grout, Cem. Concr. Aggr. 20 (1998) 145.

[30] P. Rodríguez-Lucena, J.J. Lucena, L. Hernández-Apaolaza, Relationship between the structure of Fe–lignosulfonate complexes determined by FTIR spectroscopy and their reduction by the leaf Fe reductase, The Proceedings of the International Plant Nutrition Colloquium XVI, UC Davis (2009), December 2010 http://escholarship.org/uc/item/9k69q71d, retrieved from.